Estimation of Attitude Sensor Timetag Biases ¨

J. Sedlak
Computer Sciences Corporation
Lanham-Seabrook, Maryland, USA 20706

Abstract

This paper presents an extended Kalman filter for estimating attitude sensor timing errors. Spacecraft attitude is determined by finding the mean rotation from a set of reference vectors in inertial space to the corresponding observed vectors in the body frame. Any timing errors in the observations can lead to attitude errors if either the spacecraft is rotating or the reference vectors themselves vary with time.

The state vector here consists of the attitude quaternion, timetag biases, and, optionally, gyro drift rate biases. The filter models the timetags as random walk processes: their expectation values propagate as constants and white noise contributes to their covariance. Thus, this filter is applicable to cases where the true timing errors are constant or slowly varying.

The observability of the state vector is studied first through an examination of the algebraic observability condition and then through several examples with simulated star tracker timing errors. The examples use both simulated and actual flight data from the Extreme Ultraviolet Explorer (EUVE). The flight data come from times when EUVE had a constant rotation rate, while the simulated data feature large angle attitude maneuvers. The tests include cases with timetag errors on one or two sensors, both constant and time-varying, and with and without gyro bias errors.

Due to EUVE's sensor geometry, the observability of the state vector is severely limited when the spacecraft rotation rate is constant. In the absence of attitude maneuvers, the state elements are highly correlated, and the state estimate is unreliable. The estimates are particularly sensitive to filter mistuning in this case. The EUVE geometry, though, is a degenerate case having coplanar sensors and rotation vector. Observability is much improved and the filter performs well when the rate is either varying or noncoplanar with the sensors, as during a slew. Even with bad geometry and constant rates, if gyro biases are independently known, the timetag error for a single sensor can be accurately estimated as long as its boresight is not too close to the spacecraft rotation axis.

1. Introduction

One important step in spacecraft telemetry processing is assigning timetags to each sensor measurement. Errors in these timetags can occur as constant biases due to inaccurate time offsets used in the software or as possibly time-varying errors due to problems with the sensor itself or with input/output to an onboard data buffer. Timetag errors can lead to errors in the estimated attitude if either the spacecraft is rotating or the reference vectors themselves vary with time.

This work examines the feasibility of estimating attitude sensor timetag errors along with the attitude quaternion and gyro rate bias (other calibration parameters could be included as well). The timing errors are thought of as constant biases (offsets from the true observation time), but the method also applies to slowly varying errors.

The timetag biases are appended to the system state vector and estimated using an extended Kalman filter. Section 2 describes the sensitivity matrix and state transition matrix needed as input to this algorithm. Some insight into the observability of the larger state vector is obtained by examining the observability matrix in Section 3. Results of several test cases are presented in Section 4. The tests include examples with timing errors on either one or two sensors, with and without gyro rate biases, for timespans with and without attitude maneuvers. Examples where the true bias is time-varying are also considered. Conclusions are given in Section 5.

2. Theory

The extended Kalman filter theory, as applied to attitude and gyro bias estimation, is given in Reference 1. One distinguishes the full state vector consisting of the quaternion and gyro bias, from the error state consisting of a small angle rotation vector, $\vec{a}$, and a correction to the gyro bias, $\Delta \vec{b}$. For each sensor measurement, the resulting error state updates the prior estimate of the full state: it rotates the attitude and additively corrects the gyro bias. Between measurements, the full state is propagated using bias-corrected gyro data.

This approach moves the normalization constraint on the attitude quaternion onto the 4th component of the error quaternion. (The error quaternion is the quaternion corresponding to the rotation vector $\vec{a}$. It automatically has 4th component equal to unity, to first order in $\vec{a}$.) This leaves the three components of $\vec{a}$ completely unconstrained, and the normal extended Kalman filter theory then is applicable.

References 2 and 3 describe the unit vector filter (UVF) observation model used here. In this model, the actual measured quantities are converted into unit vectors in the body frame before being handed to the Kalman filter. The effective sensor noise is taken to be isotropic; that is, a single scalar parameter represents the strength of the noise, regardless of the direction of the unit vector in the actual sensor field of view.

The rest of this section expands the UVF to include timetag biases by developing the sensitivity matrix and the state transition matrix. The sensitivity matrix relates the unit vector observations to the error state. It is needed at each sensor measurement to construct the Kalman gain and estimate a new error state. The state transition matrix is used to propagate the covariance of the error state between observations.

Sensitivity Matrix

The observation of a vector quantity (*e.g.*, a star unit vector) is modeled as a reference vector, $\vec{v}$, rotated into the body frame at the true time of measurement, plus random, zero-mean sensor noise, $\vec{n}_k$. The attitude matrix, A_{true}, rotates vectors from the inertial frame to the body frame representation. The predicted observation uses the attitude estimate conditioned on the prior observations

$$true \ observation \ = \ \vec{w}_{true} \ = \ A_{true}\vec{v}_{true} + \vec{n}_k$$
$$predicted \ observation \ = \ \vec{w}_{k|k-1} \ = \ A_{k|k-1}\vec{v}_k \tag{1}$$

The $k|j$ notation indicates a quantity estimated using observation data through time t_j, and propagated (if $k \neq j$) to time t_k. Thus, in the usual parlance, $k|k-1$ indicates an a priori estimate and $k|k$ an a posteriori estimate.

The observation is assigned timetag t_k, whereas the true time of the measurement is $t_{true} = t_k - \tau$. In particular, τ is the time bias to be estimated.

The true timetag bias, its estimate, and the time bias error are related as $\tau = \tau_{k|k-1} + \Delta\tau$. At each update, one estimates $\Delta\tau$ and adds it to $\tau_{k|k-1}$ to get the a posteriori $\tau_{k|k}$. This propagates as a constant to the next update time, becoming $\tau_{k+1|k}$.

To simplify the notation, one can absorb the prior estimate $\tau_{k|k-1}$ into t_k. The reference vectors always are obtained for corrected times using the best current time bias estimate, so the subscript-k properly should indicate variables at that corrected time. Specifically, t_k is corrected and replaced hereafter by $t_k - \tau_{k|k-1}$, and the time bias *error* becomes

$$\Delta\tau \ = \ t_k - t_{true} \tag{2}$$

The advantage is that only $\Delta\tau$ (and not $\tau_{k|k-1}$) need appear in the following derivation.

The attitude at (corrected) time t_k is related to the attitude at the true observation time by

$$A_k = R_A(\Delta \tau) A_{true} \qquad (3)$$

where $R_A(\Delta \tau)$ is the rotation matrix for any spacecraft motion during time $\Delta \tau$. One can represent this rotation by

$$R_A(\Delta \tau) = e^{-[\vec{\omega}_k \Delta \tau \times]} \qquad (4)$$

where the true rate, $\vec{\omega}_k$, is the gyro output, $\vec{u}_k$, corrected for the gyro bias

$$\vec{\omega}_k = \vec{u}_k - \vec{b}_k \qquad (5)$$

The estimate $\vec{\omega}_{k|k-1} = \vec{u}_k - \vec{b}_{k|k-1}$ is used to approximate $\vec{\omega}_k$ in Equation (4). Also, for any vector $\vec{v}$, the "cross-product matrix" is defined

$$[\vec{v}\times] \equiv \begin{bmatrix} 0 & -v_z & v_y \\ v_z & 0 & -v_x \\ -v_y & v_x & 0 \end{bmatrix} \qquad (6)$$

The reference vector also may vary during the time interval. Its magnitude does not contribute information to the state estimate, so only rotations need be considered. Thus, the reference vector at time t_k is related to the reference at the true observation time by

$$\vec{v}_k = R_v(\Delta \tau) \vec{v}_{true} \qquad (7)$$

If the reference vector is rotating at a mean rate $\vec{r}_k$, then

$$R_v(\Delta \tau) = e^{[\vec{r}_k \Delta \tau \times]} \qquad (8)$$

The sign in the exponent here is opposite to that in Equation (4) because R_v refers to actual rotation of a vector rather than its apparent motion due to rotation of the body frame.

The sign of the attitude error angle $\vec{\alpha}$ is defined such that the true and estimated attitude matrices at time t_k are related by

$$A_k = e^{[\vec{\alpha}_k \times]} A_{k|k-1} \qquad (9)$$

The seven-component state error vector is

$$x_k = \begin{bmatrix} \vec{\alpha}_k \\ \Delta \vec{b}_k \\ \Delta \tau_k \end{bmatrix} \qquad (10)$$

381

The sensitivity matrix, H_k, is the derivative of the observation with respect to the state, evaluated at the prior state estimate. One can also write this as a relationship between the observation residual, $\vec{y}_k$, and the error state

$$\vec{y}_k = H_k x_k + \vec{n}_k \tag{11}$$

Note that the a priori *error* state is identically zero since it already has been used to update the *full* state vector after the previous observation (the actual error may be nonzero, but its estimate vanishes). Expanding $\vec{y}_k$ to lowest order in the error components (expanding about zero) yields

$$
\begin{aligned}
\vec{y}_k &= \vec{w}_{true} - \vec{w}_{k|k-1} \\
&= A_{true}\vec{v}_{true} + \vec{n}_k - A_{k|k-1}\vec{v}_k \\
&\approx \left(I + [\vec{\omega}_k \Delta\tau_k \times]\right)\left(I + [\vec{\alpha}_k \times]\right) A_{k|k-1}\left(I - [\vec{r}_k \Delta\tau_k \times]\right)\vec{v}_k - \vec{w}_{k|k-1} + \vec{n}_k \\
&\approx -[\vec{w}_{k|k-1} \times]\vec{\alpha}_k - \vec{w}_{k|k-1} \times \vec{\omega}_{k|k-1}\Delta\tau_k - A_{k|k-1}(\vec{r}_k \times \vec{v}_k)\Delta\tau_k + \vec{n}_k \\
&= -[\vec{w}_{k|k-1} \times]\vec{\alpha}_k - \vec{w}_{k|k-1} \times \left(\vec{\omega}_{k|k-1} - A_{k|k-1}\vec{r}_k\right)\Delta\tau_k + \vec{n}_k
\end{aligned} \tag{12}
$$

Thus, the sensitivity matrix is

$$H_k = \begin{bmatrix} -[\vec{w}_{k|k-1} \times] & 0_{3\times3} & -\vec{w}_{k|k-1} \times \left(\vec{\omega}_{k|k-1} - A_{k|k-1}\vec{r}_k\right) \end{bmatrix} \tag{13}$$

If one simultaneously observes two vectors, $\vec{w}^1$ and $\vec{w}^2$, (*e.g.*, using two star trackers) to estimate the timetag bias of only $\vec{w}^1$, one obtains

$$H_k = \begin{bmatrix} -[\vec{w}^1 \times] & 0_{3\times3} & -\vec{w}^1 \times (\vec{\omega} - A\vec{r}) \\ -[\vec{w}^2 \times] & 0_{3\times3} & 0_{3\times1} \end{bmatrix} \tag{14}$$

where all quantities are a priori estimates $(k|k-1)$.

State Transition Matrix

The time evolution of the attitude and gyro bias parts of the error state is described in References 1 and 3. The attitude error is rotated at the rate $\vec{\omega}$, with a correction due to the gyro bias error and a noise term. The gyro and timetag biases are represented using random walk models. The timetag bias may be more properly modeled as a random constant, but the random walk leads to a somewhat more robust filter and prevents the covariance from underflowing. The evolution equation is

$$\frac{dx}{dt} = Fx + \eta$$

$$
= \begin{bmatrix} -[\vec{\omega} \times] & I_{3\times3} & 0_{3\times p} \\ 0_{3\times3} & 0_{3\times3} & 0_{3\times p} \\ 0_{p\times3} & 0_{p\times3} & 0_{p\times p} \end{bmatrix}\begin{bmatrix} \vec{\alpha} \\ \Delta\vec{b} \\ \Delta\vec{\tau} \end{bmatrix} + \begin{bmatrix} \vec{\eta}_\alpha \\ \vec{\eta}_b \\ \vec{\eta}_\tau \end{bmatrix} \tag{15}
$$

where $\Delta\vec{\tau}$ here is written more generally as a p-component vector, representing timetag bias errors for p different sensors. The vector, η, is the white noise source driving random walks in the attitude, gyro bias, and timetag bias.

Assuming the angular rates are constant during the propagation time interval, $\Delta t = t_2 - t_1$, the transition matrix is the exponential of the evolution matrix F times Δt:

$$\Phi(t_2,t_1) \equiv \Phi(\Delta t) = e^{F\Delta t} = \begin{bmatrix} \phi & \psi & 0_{3\times p} \\ 0_{3\times 3} & I_{3\times 3} & 0_{3\times p} \\ 0_{p\times 3} & 0_{p\times 3} & I_{p\times p} \end{bmatrix} \tag{16}$$

with

$$\phi(t) = \sum_{j=0}^{\infty} (-[\vec{\omega}\times])^j \frac{t^j}{j!} \tag{17}$$

and

$$\psi(t) = \sum_{j=0}^{\infty} (-[\vec{\omega}\times])^j \frac{t^{j+1}}{j+1!} \tag{18}$$

These sums collapse into well-known, finite expressions for ϕ and ψ (*e.g.*, Reference 4). Finally, the transition matrix, along with the process noise Q-matrix obtained from η, is used to propagate the state error covariance over the time interval Δt (References 4 and 5).

3. Observability

The observability condition for an nth-order, constant coefficient, deterministic, discrete system is that the matrix

$$\mathcal{H} \equiv \begin{bmatrix} H \\ H\Phi \\ H\Phi^2 \\ \vdots \\ H\Phi^{n-1} \end{bmatrix} \tag{19}$$

be of rank n (Reference 5). If there are two vector observations (six components) per update as in Equation (14), $\mathcal{H}$ will have dimension $6n \times n$; the rank n requirement then is that there be an $n\times n$ nonsingular submatrix (*i.e.*, its n remaining rows or columns must be independent after deleting $5n$ of its $6n$ rows).

This can be related to the batch solution for the epoch value of a state vector, x_o. The state is observable if x_o is uniquely determined by a set of n distinct observations, $\vec{y}_k$, made on x_o and the propagated states $\Phi^k x_o$. From Equations (11) and (19) one has

$$\begin{bmatrix} \vec{y}_0 \\ \vec{y}_1 \\ \vdots \\ \vec{y}_{n-1} \end{bmatrix} = \mathcal{H} x_o \tag{20}$$

where the noise term has been dropped (it is not usually important for observability). Left multiplication by $\mathcal{H}^T W$, where W is an arbitrary, positive-definite weight matrix, yields an $n \times n$ square matrix, $\mathcal{H}^T W \mathcal{H}$, on the right hand side. Now, if $\mathcal{H}$ has full rank, $\mathcal{H}^T W \mathcal{H}$ can be inverted to obtain

$$x_o = \left(\mathcal{H}^T W \mathcal{H}\right)^{-1} \mathcal{H}^T W \begin{bmatrix} \vec{y}_0 \\ \vec{y}_1 \\ \vdots \\ \vec{y}_{n-1} \end{bmatrix} \tag{21}$$

and x_o is recovered.

When the attitude, gyro bias, and a timetag bias for a single sensor ($p = 1$) are estimated, there are $n = 7$ error state components, and one obtains from Equations (14), (16), and (19)

$$\mathcal{H} = - \begin{bmatrix} [\vec{w}^1 \times] & 0 & \vec{w}^1 \times \vec{\omega} \\ [\vec{w}^2 \times] & 0 & 0 \\ [\vec{w}^1 \times]\phi & [\vec{w}^1 \times]\psi & \vec{w}^1 \times \vec{\omega} \\ [\vec{w}^2 \times]\phi & [\vec{w}^2 \times]\psi & 0 \\ [\vec{w}^1 \times]\phi^2 & [\vec{w}^1 \times](\phi\psi+\psi) & \vec{w}^1 \times \vec{\omega} \\ \vdots & \vdots & \vdots \\ [\vec{w}^1 \times]\phi^{n-1} & [\vec{w}^1 \times]\sum_{j=0}^{n-2}\phi^j\psi & \vec{w}^1 \times \vec{\omega} \\ [\vec{w}^2 \times]\phi^{n-1} & [\vec{w}^2 \times]\sum_{j=0}^{n-2}\phi^j\psi & 0 \end{bmatrix} \tag{22}$$

where the reference vector time derivative, $\dot{\vec{r}}$, has been assumed negligible.

Note that the assumption of a constant coefficient system was made to keep Equation (19) simple. Thus, the vectors $\vec{w}^1$ and $\vec{w}^2$ were taken to be the same after each propagation. But if they are constant in the body frame, they must refer to different inertial frame vectors (assuming $\phi \neq I$). So, Equation (22) represents the state observability after measuring n distinct vector pairs.

To make sense of Equation (22), evaluate it explicitly for a set of vectors with a geometry similar to that for the Extreme Ultraviolet Explorer (EUVE). Let

$$\vec{\omega} = (\omega, 0, 0)^T$$

$$\vec{w}^1 = (1, 1, 0)^T / \sqrt{2} \tag{23}$$

$$\vec{w}^2 = (-1, 1, 0)^T / \sqrt{2}$$

and assume Δt is small to simplify ϕ and ψ. Then,

$$\mathcal{H} \approx \frac{-1}{\sqrt{2}} \begin{bmatrix}
0 & 0 & 1 & 0 & 0 & 0 & 0 \\
0 & 0 & -1 & 0 & 0 & 0 & 0 \\
-1 & 1 & 0 & 0 & 0 & 0 & -\omega \\
\\
0 & 0 & 1 & 0 & 0 & 0 & 0 \\
0 & 0 & 1 & 0 & 0 & 0 & 0 \\
-1 & -1 & 0 & 0 & 0 & 0 & 0 \\
\\
0 & -\omega\Delta t & 1 & 0 & 0 & \Delta t & 0 \\
0 & \omega\Delta t & -1 & 0 & 0 & -\Delta t & 0 \\
-1 & 1 & \omega\Delta t & -\Delta t & \Delta t & 0 & -\omega \\
\\
0 & -\omega\Delta t & 1 & 0 & 0 & \Delta t & 0 \\
0 & -\omega\Delta t & 1 & 0 & 0 & \Delta t & 0 \\
-1 & -1 & -\omega\Delta t & -\Delta t & -\Delta t & 0 & 0 \\
\\
0 & -2\omega\Delta t & 1 & 0 & 0 & 2\Delta t & 0 \\
0 & 2\omega\Delta t & -1 & 0 & 0 & -2\Delta t & 0 \\
-1 & 1 & 2\omega\Delta t & -2\Delta t & 2\Delta t & 0 & -\omega \\
& \vdots & & & \vdots & & \vdots
\end{bmatrix} \qquad (24)$$

Several features can be identified. First, if one is solving only for the attitude ($n = 3$), only the leftmost 18×3 submatrix applies. One can see that the first, third, and sixth rows are independent and span the three-component vector space. Thus, as expected, a single pair of vectors is adequate to determine an attitude (it is not necessary to use rows beyond the sixth, so additional observations are redundant).

Second, if one is solving for attitude and gyro bias ($n = 6$), the leftmost 36×6 submatrix applies. Again, rows 1, 3, and 6 span the attitude part of the state. Then rows 7, 9, and 12 span the gyro bias components. So this state is observable after two distinct observations of two vectors each.

Third, if one is solving for attitude and time bias ($n = 4$), the 24×4 submatrix consisting of the leftmost three columns and the rightmost column applies. One can span the first three components, with no admixture of the time bias column, by using rows 1, 6, and 7. Then, row 3 completes the set.

Finally, the entire 42×7 matrix has only rank 6. There do not exist seven independent rows. (This holds with the full ϕ and ψ, not just for the small Δt approximation.) The seven-component error state is not observable under the assumptions of a constant coefficient system and the EUVE-like geometry given in Equation (23). One can estimate the attitude and either the gyro bias or the timetag bias but not all three.

In Equation (23), the rotation rate and observed vectors in the body frame are coplanar. The unobservability of the seven-component system actually arises from this degeneracy. If they are noncoplanar, $\mathcal{H}$ does have the full rank 7. In addition, the state is observable if the system is time-dependent. Then, different rates effectively appear in subsequent rows, enabling all the components to be disentangled. Thus, for EUVE, slewing the spacecraft can improve observability both by introducing a time-dependence and by shifting the rotation vector out of the plane defined by the sensors.

385

4. Test Cases

This section presents test cases showing when a timetag bias can and cannot be determined, and how it affects the estimation of the rest of the state vector. Most of these results are summarized in Table 1. For all cases listed in the table, except where indicated, the state vector consists of attitude, gyro bias, and timetag bias.

The EUVE flight data cover a two-orbit timespan for December 16, 1992, when the spacecraft was in Survey Mode, rolling about the body x-axis at 3 rotations per orbit (rpo). Performance statistics reported below are obtained as mean values or root-mean-square (RMS) averages over the second orbit of the data set. The simulated EUVE data cover a 4000 sec timespan with characteristics similar to the flight data. Mean and RMS values for these cases are obtained from the second half of the timespan.

Two Timetag Biases

The UVF software was modified to solve simultaneously for separate timetag biases for the two fixed-head star trackers (FHST1 and FHST2). Simulated biases were added to the true timetags by the driver routine. Inclusion or exclusion of gyro biases in the state vector did not change these results significantly. It was found that the algorithm could not determine the time biases.

Figure 1 shows the estimated biases, their error (square root of the estimated variance), and the attitude error (root of the trace of the attitude part of the covariance matrix). The true (simulated) time biases were -0.8 and 0.0 sec. The estimates were -0.4 and 0.4 sec. The error is much larger than the estimated 1σ error of 0.06 sec. Also, the attitude error is 40 arcsec, substantially larger than the 5-arcsec errors typical of the UVF in the absence of timetag biases. In addition, the *actual* deviation between the estimated attitude and the onboard computer (OBC) estimate is 250 arcsec (RMS over the second orbit). The corresponding deviation is only 12 arcsec when no timing errors are present (Reference 4). This attitude deviation comes from the 0.4-sec average timetag error times the 3 rpo roll rate, which leads to a large roll offset. The correlation coefficients obtained from the orbit-averaged covariance matrix are near unity between the two timetags and also between the timetags and the roll angle. It is interesting that in this, and several similar test cases, the algorithm correctly obtained the difference between the FHST1 and FHST2 timetag biases to within about 0.05 sec. (This did not hold for differently placed sensors.)

Single Timetag Bias without Gyro Bias

In all subsequent tests, the filter solves for the timetag bias for only one sensor at a time. In this example, FHST2 is given a time bias of -0.3 sec. The true gyro biases are compensated using values obtained from the UVF smoother (Reference 4) and are not estimated. Figure 2 shows the estimated FHST2 timetag bias and the timetag and attitude errors derived from the covariance matrix. The time bias converges in a few hundred seconds and settles on a mean value differing from the true bias by only a few microseconds. Its estimated 1σ error is 0.005 sec (the actual standard deviation of the estimate is about 0.002 sec). The attitude estimates are very good (similar to solutions with no timing errors): estimated 1σ error is 4 arcsec, and RMS deviation from the OBC estimate is 12 arcsec. The largest correlation coefficient occurs between the timetag bias and the roll error, but its value is only 0.43. This is the only example for which the time bias estimation worked well without an attitude maneuver.

Single Timetag Bias with Gyro Bias

Figure 3 shows a case identical to that in Figure 2, except that gyro biases are also estimated. Comparison with Figure 2 indicates that the convergence is much slower, and, in fact, the time bias is moving in the wrong direction for much of the last few thousand seconds. The true simulated time bias is -0.3 sec, but the mean estimate (for the second orbit) is -0.25 sec. The estimated 1σ errors obtained from the covariance matrix are 0.02 sec, 12 arcsec, and 0.03 deg/hr

for the time bias, attitude, and gyro biases, respectively. These are significantly worse than the 5 arcsec and 0.007 deg/hr attitude and gyro bias errors obtained without timetag errors. The RMS deviation from the OBC estimate is 26 arcsec. In addition, the correlation coefficients indicate that the solution is unreliable, several being over 0.9. These results show that EUVE's attitude, gyro bias, and timetag bias together are not observable without maneuvers.

Having established that the filter can correct either the timetag or the gyro biases, but not both, iterative methods were attempted. Data with both a gyro bias and an FHST2 timetag bias were processed repeatedly, solving alternately for the gyro and the timetag bias. The results do not converge. Similarly, the iterative solution for two separate FHST timetag biases fails to converge. Thus, as expected, the observability problems that spoil the simultaneous estimation of two time biases or a timetag and gyro bias cannot be circumvented by estimating them separately and iteratively.

Timetag Bias Estimation During Maneuvers

A series of tests using simulated EUVE data were performed to show the influence of attitude maneuvers on the state observability (attitude, gyro bias, and timetag bias). The simulations include 0, 1, or 2 slews of roughly 30 deg at 0.1 deg/sec. The first slew is about the body y-axis. When there are two slews, the second is about the body z-axis. Both slews occur during the first 2000 sec.

One advantage of simulation data is that the noise characteristics are known exactly, so these tests also offer an opportunity to look briefly at the effects of filter mistuning. The filter is precisely tuned when it agrees with the simulator on the strengths of the white noise sources. These are the process noise η in Equation (15) and the sensor noise $\bar{n}$ in Equation (1). In these tests, the simulated timing error is a constant ($\eta_\tau = 0$) while the filter's timetag noise parameter is set to a small nonzero value. All other noise parameters were tuned exactly. In this case, the actual solution deviations from the true values agree very well with the expected 1σ errors. When the spacecraft undergoes maneuvers, these errors decrease in parallel. The 1σ timetag error decreases from 0.024 to 0.009 to 0.006 sec for 0, 1, and 2 slews, while the actual mean deviations go from 0.021 to 0.012 to 0.004 sec (see Table 1). The attitude errors and RMS deviations from the truth model both decrease from 14 to 7 to 5 arcsec. Most importantly, the largest correlation coefficient decreases from near unity to 0.77 for the two slew case, indicating that the separate state components have become distinguishable.

When the filter is mistuned, the 1σ errors and actual deviations no longer agree so closely. For this test, the FHST noise parameter was set to 0.005 deg rather than the true 0.01 deg used in the simulator. This causes the expected errors to decrease while the mistuning should cause the actual deviations to increase. With no maneuvers, this is exactly what is found. The timetag deviation increases to 0.032 sec and the attitude deviation increases to 18 arcsec. What is interesting is that with two slews the solution is much less sensitive to this mistuning. In this case, the actual errors revert to near their tuned values, 0.004 sec and 5 arcsec. (Some degradation is expected, but this can only be seen by averaging results from many runs using different random number sequences and initial conditions.) One concludes that state observability is an important part of filter robustness.

Estimation of Variable Timetag Bias

For the final tests, the filter is asked to solve for a single, but time-varying, timetag bias. A sawtooth function with amplitude -0.5 sec and a period of either 60 sec or 3000 sec is added to the true FHST1 timetag. Gyro biases are not estimated; the rates are corrected using the true gyro biases, determined separately.

If the filter memory time is too long, it will not be able to follow a varying time bias; it will converge instead to an average value. The process noise needs to be large enough to produce an uncertainty roughly comparable to the sawtooth amplitude in a time equal to the period. The timetag process noise is characterized by the parameter σ_τ^2, obtained from

the two-time expectation of the white noise source η_τ appearing in Equation (15):

$$E\left[\eta_\tau(t)\,\eta_\tau(t')\right] = \sigma_\tau^2\,\delta(t-t') \qquad (25)$$

A range of values for σ_τ^2 from 0.01 to 0.001 sec²/sec leads to similar results. (All other test cases where the timetag biases were constant used $\sigma_\tau^2 = 10^{-8}$ sec²/sec.)

Figure 4 shows the timetag bias from a typical 400-sec timespan for the more rapidly varying case. The estimate is shown as a solid line and the true timing error as a sawtooth dashed line. When the observability is good (stars available in both trackers), the estimated bias can follow the sawtooth with a residual of roughly 0.05 sec or less. However, the overall performance is not very good since the sawtooth quickly moves away from the estimated time bias between star identifications.

In spite of the rather poor timetag estimation, inclusion of the time bias in the state vector does improve the attitude determination significantly. The RMS deviation from the OBC attitude is only 11 arcsec, as good as tests with no timing errors. Without time bias estimation, the sawtooth timing error causes an RMS attitude deviation of 74 arcsec.

When the period of the sawtooth is increased to 3000 sec, the filter has much less trouble following it. Figure 5 shows the timetag bias estimate (solid) and the slowly varying true bias (dashed). The RMS deviation from the OBC is 11.5 arcsec in this case.

5. Conclusions

It has been shown that, without maneuvers, attitude sensor timing errors onboard EUVE and spacecraft with similar geometry can be solved for only for very limited circumstances. Examination of the $\mathcal{H}$-matrix shows that the attitude, gyro bias, and timetag bias are not simultaneously observable. A Kalman filter solution leads to results with large correlation coefficients. These solutions are not robust: filter mistuning changes the results and iterative methods lead to radically different estimates or diverge altogether. The timetag bias can be accurately determined only if the gyro bias is not solved for and is compensated using an accurate independent estimate.

Similarly, when there are timetag errors on two sensors, the filter algorithm cannot distinguish them. Large correlations between the individual sensors' timetag biases indicate that their estimates are unreliable. Additional tests are needed to examine cases with three or more sensors, with and without attitude maneuvers.

The observability improves dramatically when the spacecraft undergoes attitude maneuvers. The correlation coefficients decrease and the state estimates improve for each slew. This only holds, though, with fairly large maneuvers. Tests with recent EUVE flight data having a pair of 2 deg slews showed no noticeable increase in observability.
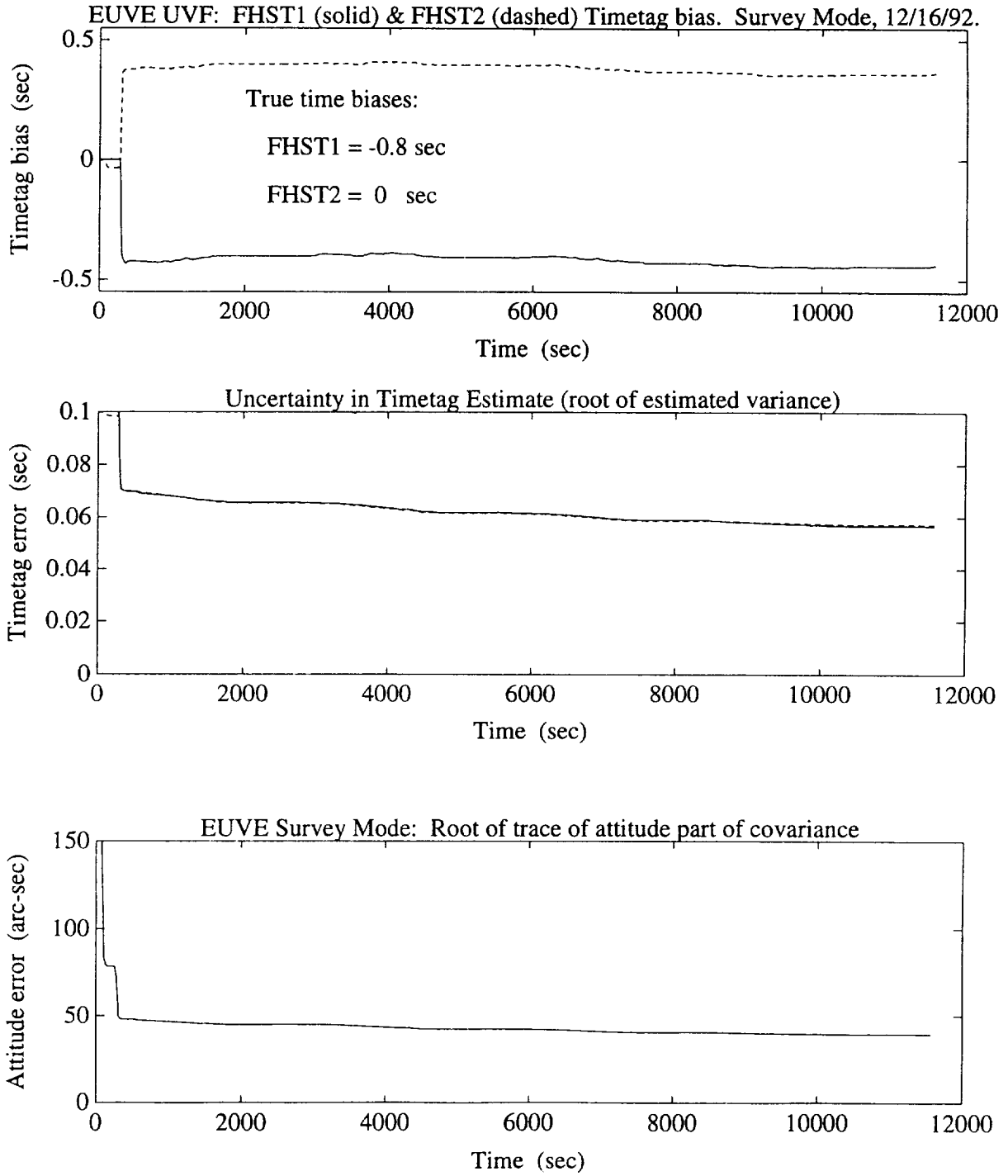
Even when the gyro bias has been compensated, the filter does not do well estimating a short-period, time-varying timetag bias. However, the problem here is probably insufficient data relative to the bias time scale (period equal to 1 minute in this test case). The filter has no trouble following the long-period variations in the final test. In either case, estimating the timetag bias improved the attitude estimates significantly. If a particular sensor has a known short-period timing problem, a better sensor model could be developed to estimate, for example, the period, amplitude, and phase as three new state vector elements, rather than trying to follow the time-variation using a single timetag bias with a large process noise.

Table 1. Timetag Bias Filter Statistics

| Test Cases	Mean Timetag Deviation from True (sec)	Estimated Timetag 1σ Error (sec)	RMS Attitude Deviation from True (arcsec)	Estimated Attitude 1σ Error (arcsec)	Largest Correlation Coefficient
No Timing Error	NA	NA	11.8	5.0	0.62
One Timetag (w/o Gyro Bias)	< 5.E-06	0.005	12.0	4.2	0.43
One Timetag	0.052	0.020	25.8	12.4	0.97
Two Timetags	0.4	0.06	247	40	0.99
Simulation with No Maneuvers	0.021	0.024	13.5	13.9	0.98
Simulation with One Maneuver	0.012	0.009	6.9	6.5	0.85
Simulation with Two Maneuvers	0.004	0.006	5.1	5.1	0.77
Simulation with No Maneuver - Mistuned Filter	0.032	0.010	18.4	7.4	0.96
Simulation with Two Maneuvers - Mistuned Filter	0.004	0.004	4.8	3.6	0.65

References

1. E. J. Lefferts, F. L. Markley, and M. D. Shuster, "Kalman Filtering for Spacecraft Attitude Estimation," *J. Guidance, Control, and Dynamics*, Vol. 5, No. 5, Sept.-Oct. 1982, pp. 417-429

2. M. D. Shuster, "Kalman Filtering of Spacecraft Attitude and the QUEST Model," *J. Astronaut. Sci.*, Vol. 38, No. 3, July-Sept. 1990

3. J. Sedlak and D. Chu, "Kalman Filter Estimation of Attitude and Gyro Bias with the QUEST Observation Model," in *Proceedings, AAS/GSFC International Symposium on Space Flight Dynamics*, April 1993

4. J. Sedlak, "Comparison of Kalman Filter and Optimal Smoother Estimates of Spacecraft Attitude," in *Proceedings, Flight Mechanics/Estimation Theory Symposium*, NASA Goddard Space Flight Center, May 1994

5. A. Gelb, ed., *Applied Optimal Estimation*, MIT Press, Cambridge, MA, 1974

EUVE UVF: FHST1 (solid) & FHST2 (dashed) Timetag bias. Survey Mode, 12/16/92.

True time biases:

FHST1 = -0.8 sec

FHST2 = 0   sec

Uncertainty in Timetag Estimate (root of estimated variance)

EUVE Survey Mode: Root of trace of attitude part of covariance

Figure 1. Timetag Biases, Timetag Errors, and Attitude Error When Estimating Timetag Biases for Two Sensors
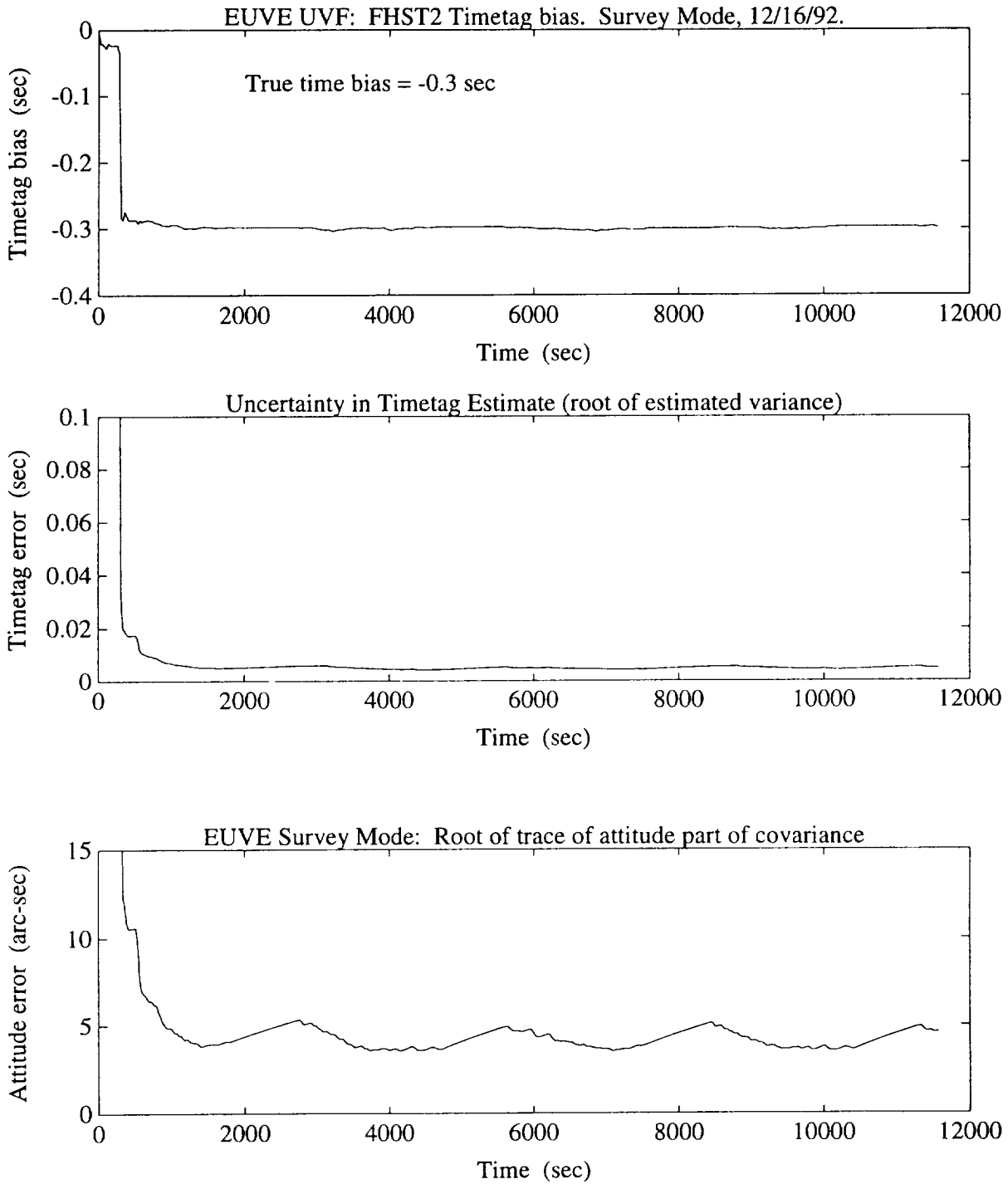
Figure 2. *Timetag Bias, Timetag Error, and Attitude Error When Estimating Timetag Bias for a Single Sensor*
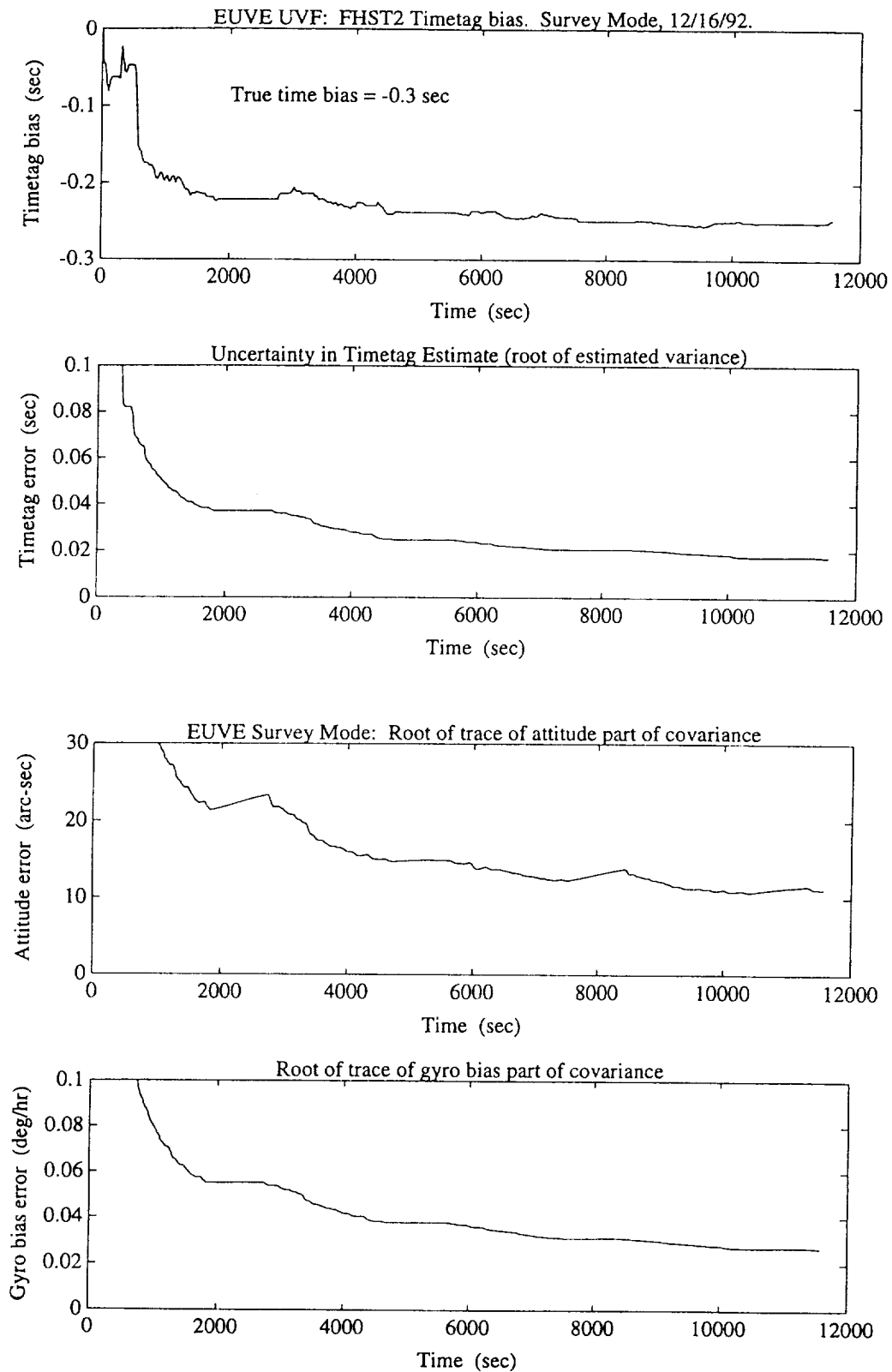
Figure 3. Timetag Bias, Timetag Error, Attitude Error, and Gyro Bias Error When Estimating Gyro Biases and Timetag Bias for a Single Sensor

(detail): Estimated (solid) & true timetag bias (dashed)
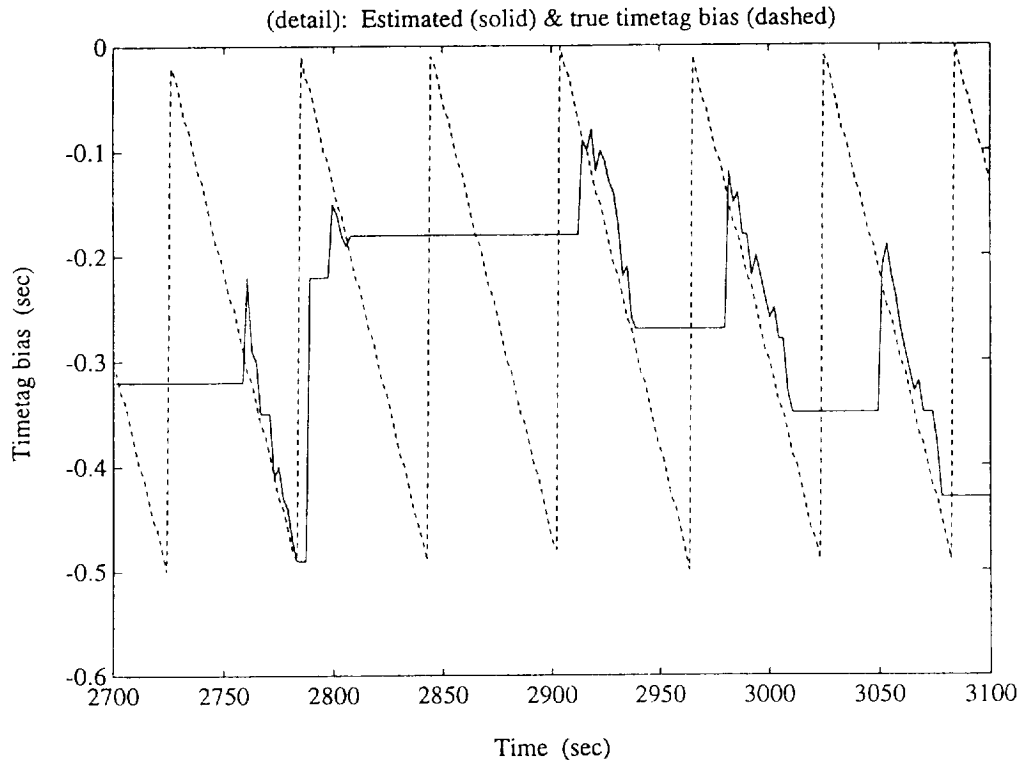
Figure 4. Estimated and True Timetag Biases When Estimating a Rapidly Varying Timetag for a Single Sensor

EUVE UVF: FHST1 timetag bias (true bias = sawtooth). Survey Mode, 12/16/92.
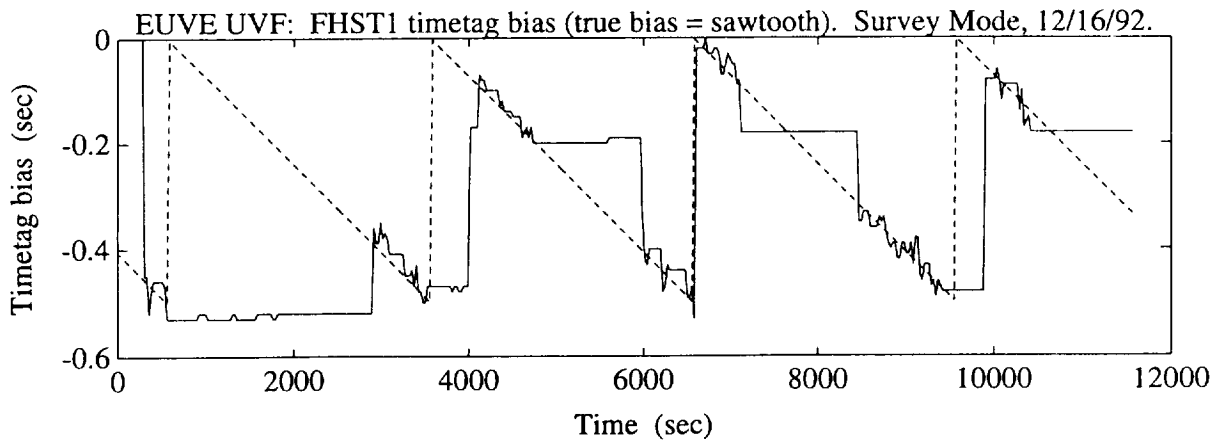
Figure 5. Estimated and True Timetag Biases When Estimating a Slowly Varying Timetag for a Single Sensor

393